Title

The New CLOCIT Irradiation Facility for 40Ar/39Ar Geochronology: Characterisation, Comparison with CLICIT and Implications for High-Precision Geochronology

Journal

Geostandards and Geoanalytical Research, 42(3)

ISSN

1639-4488

Authors

Rutte, Daniel
Becker, Tim A
Deino, Alan L
et al.

Publication Date

2018-09-01

DOI

10.1111/ggr.12217

Peer reviewed

Vol. 42 — N° 3 09 18 p. 301 – 307

GEOSTANDARDS and GEOANALYTICAL RESEARCH

The New CLOCIT Irradiation Facility for $^{40}Ar/^{39}Ar$ Geochronology: Characterisation, Comparison with CLICIT and Implications for High-Precision Geochronology

Daniel **Rutte** (1, 2)*, Tim A. **Becker** (1), Alan L. **Deino** (1), Steven R. **Reese** (3), Paul R. **Renne** (1, 2) and Robert A. **Schickler** (3)

(1) Berkeley Geochronology Center, Berkeley, CA, USA
(2) Department of Earth and Planetary Science, University of California, Berkeley, CA, USA
(3) Nuclear Science and Engineering, Oregon State University, Corvallis, OR, USA
* Corresponding author. e-mail: d.rutte@gmx.de

The Cadmium-Lined Outer-Core Irradiation Tube (CLOCIT) is a new irradiation facility for $^{40}Ar/^{39}Ar$ geochronology at the Oregon State University TRIGA® reactor. We report fluence (i.e., time-integrated flux) parameters from the first four CLOCIT irradiations and compare them with the existing Cadmium-Lined Inner-Core Irradiation Tube (CLICIT). CLOCIT provides an average neutron flux equivalent of 1.45–1.53 × 10^{-4} *J* h^{-1}; about 55% of CLICIT. Radial fluence gradients were on the order of 0.2–4.2% cm^{-1}. A planar fit of *J*-values results in residuals in the range of uncertainty in the *J*-value, but systematic deviations resolve a non-planar component of the neutron flux field, which has also been observed in CLICIT. Axial neutron fluence gradients were 0.6–1% cm^{-1}, compared with 0.7–1.6% cm^{-1} for the CLICIT. Production rate ratios of interfering reactions were $(^{40}Ar/^{39}Ar)_K$ = (4 ± 6) × 10^{-4} and $(^{38}Ar/^{39}Ar)_K$ = (1.208 ± 0.002) × 10^{-2}, $(^{36}Ar/^{37}Ar)_{Ca}$ = (2.649 ± 0.014) × 10^{-4}, $(^{38}Ar/^{37}Ar)_{Ca}$ = (3.33 ± 0.12) × 10^{-5} and $(^{39}Ar/^{37}Ar)_{Ca}$ = (9.1 ± 0.28) × 10^{-4}, similar to the CLICIT values.

Keywords: Ar-Ar dating, geochronology, reference materials, argon isotopes, neutron fluence gradient, nuclear reactions, research reactor.

Received 14 Feb 18 – Accepted 27 Apr 18

The Cadmium-Lined Inner-Core Irradiation Tube (CLICIT) in the TRIGA® reactor at Oregon State University (OSU) is a highly utilised irradiation facility for $^{40}Ar/^{39}Ar$ geochronology. In 2017, 79 irradiations were conducted for twenty-three laboratories from twelve different countries. Increased CLICIT demand has led to sample backlogs of up to 300 h with OSU limited to 35 h of operation a week. Responding to demand, a second facility, the Cadmium-Lined Outer-Core Irradiation Tube (CLOCIT), has been commissioned. Here, we report results from the first four irradiations spanning 17 min to 32.25 h to characterise the new facility. We document average $^{39}Ar_K$ production rates, neutron fluence gradients and production rate ratios of interference reactions on Ca and K. We compare these values with data from four recent CLICIT irradiations and production rate ratios on Ca and K established over the long term.

Technical specifications

The CLOCIT is identical in construction to the CLICIT (Schickler *et al.* 2013). It consists of two aluminium tubes: the inner tube has an outer diameter (OD) of 31.75 mm with a wall thickness of 1.47 mm. Surrounding the bottom of the inner tube is an outer tube which is 37.5 mm OD with a wall thickness of 1.45 mm. This outer tube is 1067 mm long and serves as the facility's in-core terminus. To minimise thermal neutron penetration into the irradiation facility, a 0.508 mm thick cadmium sleeve is wrapped around the outside of the inner aluminium tube and a disc of cadmium is placed at its bottom (Schickler *et al.* 2013). The facility allows irradiation of cylindrical packages with an OD of 22.86 mm and a height of 101.6 mm. The radial orientation is currently uncontrollable.

doi: 10.1111/ggr.12217

A Monte Carlo *n*-particle (MCNP) transport model of the reactor was employed to identify a position for CLOCIT that provides a high fast-neutron flux at an acceptable loss of reactivity with the cadmium sleeve introduced (Schickler and Reese 2017). Position F20 near the core periphery, but still surrounded by fuel elements provides this compromise (Figure 1). Two new fuel rods were added to the core inventory and graphite rods were shuffled to minimise the loss in reactivity.

The axial flux profiles in the CLOCIT and CLICIT were determined by activation of 55 cm long Al-Au wire ($^{197}Au(n,\gamma)^{198}Au$) in a 2-min irradiation and subsequent gamma spectrometry of ^{198}Au activity. The axial flux profile is the expected bell shape (Figure 2). OSU has historically determined 20 cm above the base of the core as the desired location for irradiation of $^{40}Ar/^{39}Ar$ samples; thus a 20 cm tall installed pedestal ('saddle') ensures the samples are irradiated at the axial peak of the neutron flux. The height can be adjusted to the needs of a specific irradiation by addition of sample spacers.

Method

We determined neutron fluences by irradiation and analysis of widely used geological sanidine reference materials from the Fish Canyon Tuff (FCs; ~ 28.2 Ma) and the Alder Creek rhyolite (ACs; ~ 1.18 Ma), and calculation of *J*-values (Equation (1), Grasty and Mitchell 1966). Equation (1) shows the relation of the ratio of $^{40}Ar^*$ (radiogenic ^{40}Ar) and $^{39}Ar_K$ (^{39}Ar activated from K) in a reference material of known age *t* with the neutron fluence Φ and their abstraction as the *J*-value. ^{39}K and ^{40}K are the respective natural abundances, λ is the total decay constant of ^{40}K, λ_e its electron capture decay constant and σ the cross section of $^{39}K(n,p)^{39}Ar$ as a function of neutron energy *E*. For a detailed derivation see Grasty and Mitchell (1966).

$$J = \frac{^{39}K}{^{40}K}\frac{\lambda}{\lambda_e}\int \Phi(E)\sigma(E)dE = \frac{e^{\lambda t}-1}{\frac{^{40}Ar^*}{^{39}Ar_K}} \qquad (1)$$

Samples were irradiated in wells of variable geometry drilled in aluminium discs 18.54 mm OD. Four to six wells outlining a square, pentagon or hexagon along the edge of the disc (spanning about 15 mm across) and in some discs additional wells in the centre of the disc were loaded with 0.25–0.3 mm grains of FCs or 0.60–0.71 mm ACs. In irradiation 468 we included crushed synthetic Fe-doped (0.8% *m/m*) aluminosilicate glass with *ca.* 11.3 % *m/m* K and a grain size of 0.4–0.6 mm around the centre of level A and crushed natural fluorite with a grain size of 0.2–0.4 mm around the centre of level B. The discs were wrapped in Al foil, stacked and encapsulated in tight-fit glass tubing (preventing tilting of the discs), which in turn was encapsulated in an aluminium tube (Figure 2b).

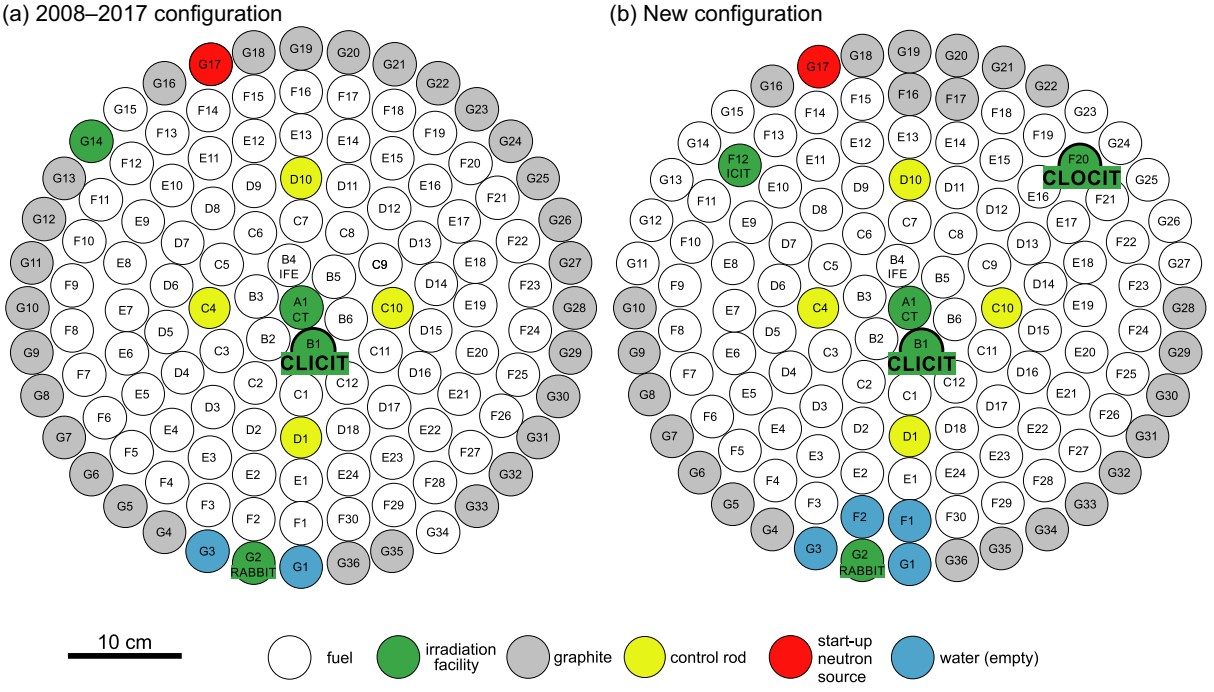

Figure 1. Diagram of the reactor core configurations (a) before and (b) after installation of the CLOCIT [Colour figure can be viewed at wileyonlinelibrary.com].

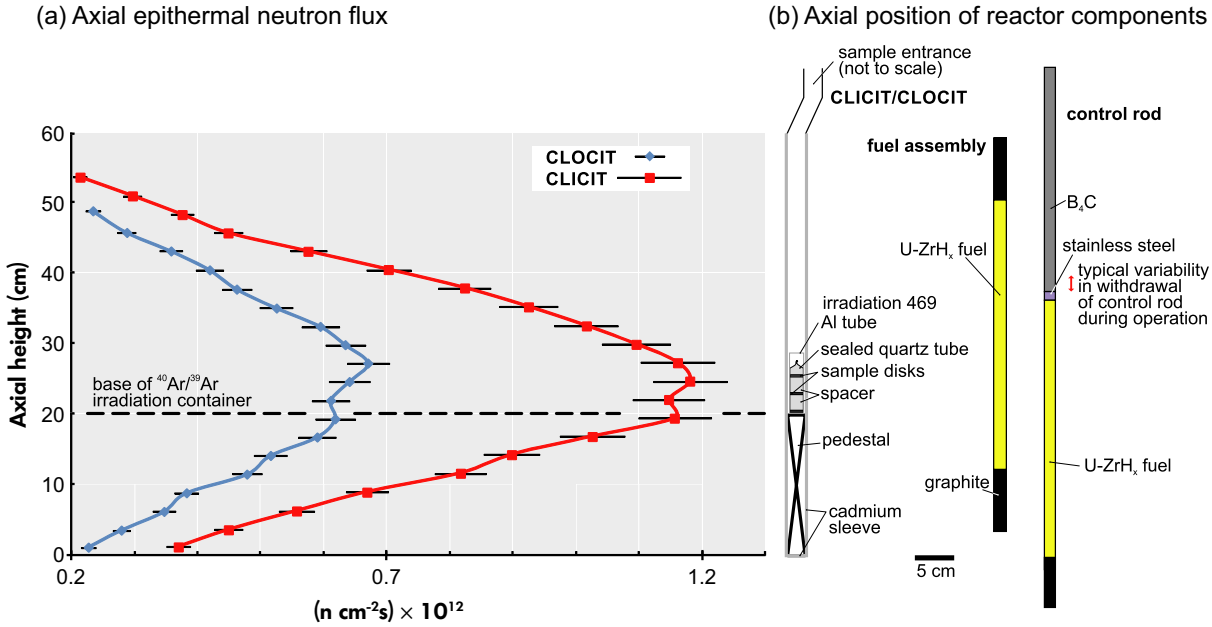

Figure 2. (a) Axial flux profile of the CLOCIT and CLICIT determined by 2-min irradiation and subsequent γ-spectrometry of Al-Au wire. The dip at ~ 22 cm axial height is likely related to operation of the control rods at this height during start-up. The dip is expected to disappear in longer irradiation times. (b) Simplified geometry and relative axial position of the relevant components of the reactor in respect to the flux profile. [Colour figure can be viewed at wileyonlinelibrary.com]

We individually analysed five to ten grains of ACs and FCs per well, heated in one or two steps and calculated an inverse-variance weighted mean (in the following 'weighted mean') *J*-value for the respective well. All three Ar analysis lines at BGC (NEXUS, MAP1 and Noblesse) were involved, using measurement routines described in Niespolo *et al.* (2017). Typical uncertainties of *J*-values of individual wells were ~ 0.15–0.4%. We determined a planar fit through the 4–8 wells of given *J*-value and calculated the deviation of each well from the fitted plane; the calculation considers uncertainty in *J*-value and predicts a *J*-value and respective uncertainty for any position. For *J*-value calculations we used ages of 28.201 Ma (Kuiper *et al.* 2008) and 1.1848 Ma (Niespolo *et al.* 2017) for FCs and ACs, respectively. Other ages are in use for these reference materials but the values used are irrelevant for the present purposes so long as they are internally consistent as was demonstrated by Niespolo *et al.* (2017).

Results and discussion

Average neutron flux

The average flux in the CLOCIT irradiations is equivalent to 1.45–1.53 × 10^{-4} *J* h^{-1} (Table 1). These values compare with 2.62–2.72 × 10^{-4} *J* h^{-1} of the last four CLICIT irradiations analysed at BGC. Thus to achieve a similar *J*-value, CLOCIT irradiations should be about 1.8 times longer than those in the CLICIT.

Fluence gradients

The axial fluence increases upwards from the basal standard irradiation position by an average of about 0.6–1% cm^{-1} in the CLOCIT, similarly the CLICIT (0.7–1.6% cm^{-1}; Table 1). For irradiation sample holders utilising wells in an aluminium disc, these gradients may be significant when reference materials and unknowns have different fill levels in the wells.

We calculated radial gradients based on planar fit through the weighted mean *J*-values of wells. The maximum deviation of individual wells from the planar fit is typically below 0.3% for both CLICIT and CLOCIT and in the range of analytical uncertainty of the *J*-value indicating that planar fits provide a decent approximation on the scale of a disc (Table 1). However, we found a systematic deviation of the central wells to lower *J*-values. The seven discs with reference materials in the central well (both CLICIT and CLOCIT irradiations) gave a weighted mean analysed-over-predicted ratio of 0.9982 ± 0.0009 (MSWD = 0.73), that is in average 0.2% lower values. Both the larger distance of the central well to the surrounding fuel elements and neutron

Table 1.
Comparison of fluence parameters of four irradiations in CLOCIT and CLICIT, respectively

Irradiation	Duration (h)	Level	*n*	Height in irradiation container (cm)	Radial gradient (% cm^{-1})	Av. unc. of *J*-values (%)	Max. dev. from planar fit (%)	Axial gradient (% cm^{-1})	$J\ h^{-1} \times 10^{-4}$
CLICIT									
468	32.25	C	4	5.3	0.87	0.18	0.01	1.0	1.53
	32.25	B	4	2.8	0.51	0.17	0.13		1.51
	32.25	A	4	0.2	0.20	0.17	0.03		1.45
470	0.28	A	4	0.2	1.15	0.23	0.26	NA	1.51
471	0.83	A	4	1.9	3.69	0.18	0.06	0.3	1.47
	0.83	B	4	1.3	4.10	0.18	0.35		1.47
	0.83	C	4	0.8	4.01	0.19	0.12		1.47
	0.83	D	5	0.2	4.24	0.24	0.15		1.46
472	5	A	4	1.9	2.17	0.10	0.01	0.6	1.47
	5	B	4	1.3	1.93	0.12	0.07		1.47
	5	C	4	0.0	1.91	0.17	0.13		1.46
	5	D	4	0.2	2.29	0.13	0.05		1.46
CLOCIT									
464	0.5	A	4	1.0	0.47	0.40	0.02	1.6	2.72
	0.5	B	4	0.2	1.23	0.30	0.25		2.68
465	2	A	4	1.0	1.07	0.41	0.31	1.4	2.65
	2	B	4	0.2	0.67	0.21	0.20		2.62
466	20	4	6	2.9	0.31	0.31	0.33	0.7	2.70
	20	3	6	2.0	0.36	0.25	0.39		2.69
	20	2	6	1.1	0.29	0.25	0.41		2.68
	20	1	6	0.2	0.45	0.32	0.30		2.65
467	1	A	6	2.9	0.07	0.49	0.22	0.9	2.70
	1	B	6	2.0	0.22	0.37	0.68		2.68
	1	C	6	1.1	0.53	0.49	0.14		2.65
	1	D	3	0.2	0.88	0.71	NA		2.64

shielding by the irradiation container and samples may contribute to this. Rutte *et al.* (2015) provide a simulated neutron flux distribution that illustrates the significantly non-planar axial variation over the irradiation channel in a comparable research reactor without an irradiation target introduced (their figure 4b). Shielding includes consumption of neutrons by capture and transfers reactions as well as neutron moderation by scattering; moderation lowers the probability of $^{39}K(n,p)^{39}Ar$ to occur due to the smaller cross section for lower energy neutrons.

These data agree with long-term observations at the Berkeley Geochronology Centre; in practice this has led to either completely avoiding extrapolating *J*-values determined from, for example outer ring reference materials to inner ring samples (Figure 3) or case to case assessment of the effects and mitigation by, for example bracketing. The following values are calculated excluding the central well as a constraint for the planar fit.

The planar fits (through the outer ring) provide a gradient in the form of $J\ cm^{-1}$; to allow comparison this was converted to % cm^{-1} for the respective centre of each disc (Figure 3, Table 1). In the four CLOCIT irradiations, radial gradients were in the range 0.2–4.2% cm^{-1}, that is up to ~ 6% variability across a single disc (Table 1). These compare with radial gradients in the CLICIT of up to 1.2% cm^{-1} (Table 1). Figure 3 shows an example of radial gradients observed in two discs irradiated in CLICIT and CLOCIT. Some irradiations display a trend with axially upward increasing radial gradients (e.g., CLOCIT irradiation 468) or axially upward decreasing radial gradients (e.g., CLICIT irradiation 467; Table 1); in both irradiations fluence increases axially upwards. In CLOCIT and CLICIT the radial gradients vary more in between irradiations than in between discs of an individual irradiation (Table 1). While higher radial gradients in CLOCIT compared with CLICIT are readily explained by the fact that it has less fuel on one side, the variability of determined axial fluence gradients between irradiations – in both facilities – is currently unknown.

Which factors may cause variability of the fluence field in between irradiations? (a) The start-up of the reactor to full power takes about 3 min and several more minutes until

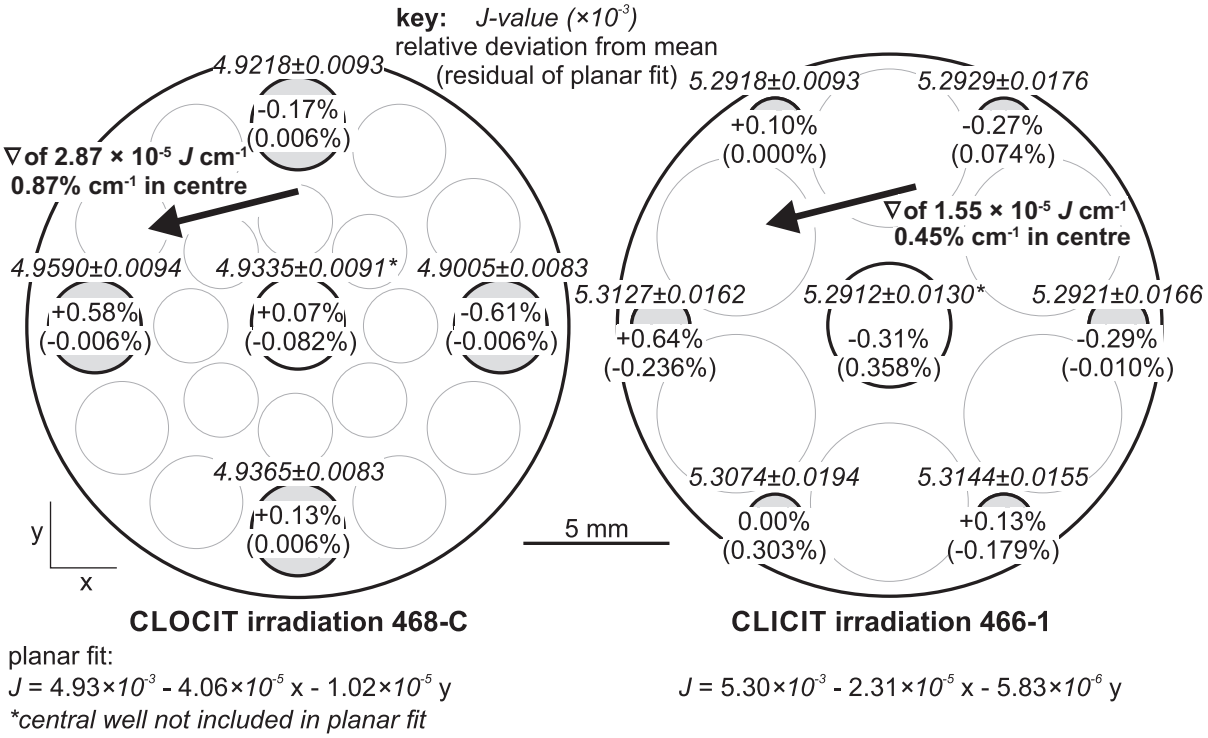

Figure 3. Maps of 21 and 13-well aluminium irradiation discs. Highlighted wells include reference materials. Weighted mean *J*-value, deviation from disc mean and residual of planar fit are indicated. Arrows trace the gradient (∇); the similar orientation is coincident. Uncertainties here and throughout are given at the 1*s* level. Point of origin is in the disc centres.

stable operation - including secular equilibration of delayed neutron precursors - is reached; the exact timing is not well known. Higher flux gradients have to be expected for this phase. In shorter irradiations, initially higher flux gradients exert greater influence on the resulting fluence gradient. This may explain the highest fluence gradients for the 50 min irradiation 471 and the smallest fluence gradients in the 32.25 h irradiation 468. However, the 16.8 min irradiation 470 with intermediate gradients suggests this cannot be the only factor. (b) Over each day and the course of a week of operation the concentration of the neutron absorber ^{135}Xe ($T_{1/2}$ = 9.2 h) increases ('Xenon poisoning') in the fuel elements and the resulting loss in criticality requires further withdrawal of the control rods. Over the course of a week this may result in about 2.5 cm difference in the insertion depth of the control rods (Figure 2b). It is unclear how this variation changes the flux field in at the sample position. (c) Contemporaneous with ^{40}Ar/^{39}Ar sample irradiation in CLOCIT, the other facilities (CLICIT, ICIT; Figure 1) are loaded with different materials that may influence the flux field in the reactor. Irradiations 471 and 472 for which we determined factor 2 different fluence gradients were irradiated in the same day, with the same irradiations continuing in CLICIT and ICIT suggesting this factor cannot explain their variability. Irradiation 471 was undertaken in the afternoon with the control rods being 0.8 cm more withdrawn compared with 472 in the morning.

For the irradiation employed herein on aluminium discs we found four reference materials on the outer ring to be sufficient to predict *J*-values on that outer ring in CLICIT. Depending on the scope of the study a higher density may be advisable for CLOCIT. For studies requiring highest precision such as reference material intercalibration CLICIT should, with current knowledge, be preferred over CLOCIT. Given the larger gradients in CLOCIT, the size of wells in discs should be limited; for example, individual crystals in a well with 5 mm diameter may experience 2% different fluence resulting in over-dispersion of single crystal ages. While the planar fit could provide satisfactory accuracy for most applications, the highest precision could be achieved by mixing reference materials and unknowns in a single well given a sufficient age difference and single grain analysis to enable distinction between reference materials and unknowns after the irradiation. With very similar axial gradients compared to CLICIT, CLOCIT provides the same qualities for stacked irradiations where samples and unknowns are arranged in line.

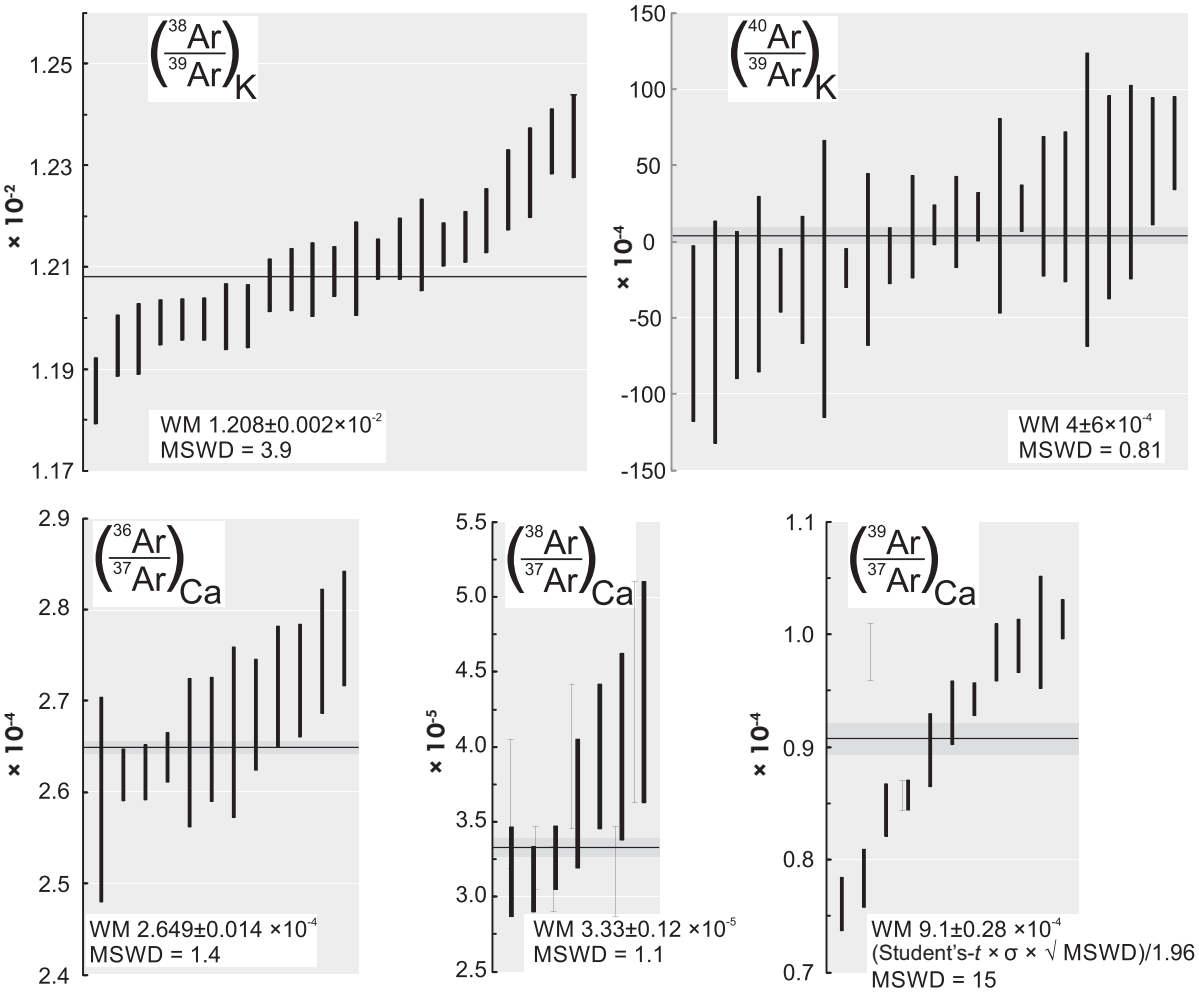

Figure 4. Ratios of Ar isotope production rates from K and Ca in CLOCIT determined from irradiated K-rich glass and fluorite (CaF_2).

Interference reactions

^{40}Ar and ^{39}Ar from K: The production ratios of $(^{40}Ar/^{39}Ar)_K$ and $(^{38}Ar/^{39}Ar)_K$, which are produced via $^{39}K(n,p)^{39}Ar$, $^{40}K(n,p)^{40}Ar$, $^{39}K(n,d)^{38}Ar$ and $^{41}K(n,\alpha\beta^-)^{38}Ar$ reactions, were determined. We analysed CLOCIT-irradiated K-rich glass by single-step-fusion of 3–8 grains. Twenty-three aliquots yielded a weighted mean of $(4 \pm 6) \times 10^{-4}$ for $(^{40}Ar/^{39}Ar)_K$ and $(1.208 \pm 0.002) \times 10^{-2}$ for $(^{38}Ar/^{39}Ar)_K$ (Figure 4). These values are indistinguishable from $(7.3 \pm 0.9) \times 10^{-4}$ and $(1.196 \pm 0.013) \times 10^{-2}$ for CLICIT (Renne *et al.* 2005). Long-term repetition of this experiment would be required to reduce uncertainty of the determined value for $(^{40}Ar/^{39}Ar)_K$, which is challenging to analyse precisely due to the low $^{40}Ar_K$ production rate in Cd-shielded irradiations. Determined ion beam intensities are provided in the online supporting informaton Table S2.

^{36}Ar, ^{37}Ar, ^{38}Ar and ^{39}Ar from Ca: We determined the production ratios of $(^{36}Ar/^{37}Ar)_{Ca}$, $(^{38}Ar/^{37}Ar)_{Ca}$ and $(^{39}Ar/^{37}Ar)_{Ca}$, which are mainly produced via $^{40}Ca(n,n\alpha)^{36}Ar$, $^{40}Ca(n,\alpha)^{37}Ar$, $^{42}Ca(n,n\alpha)^{38}Ar$, $^{43}Ca(n,n\alpha)^{39}Ar$, $^{42}Ca(n,\alpha)^{39}Ar$ and $^{43}Ca(n,n\alpha)^{39}Ar$. Fluorite irradiated in CLOCIT by single-step-fusion with a CO_2 laser was analysed. Fluorite is semi-transparent to the ~ 10 µm wavelength of the laser so it was co-loaded with previously degassed and crushed basalt glass which co-fused the fluorite when heated. Eleven aliquots of five to fifteen grains each were analysed. In contrast to the other isotopes, ^{39}Ar signals were only 10–30 times above background for most of the aliquots. The rise rates of the ^{39}Ar beam were significantly larger than those of the background measurements due to memory effects in the mass spectrometer. The calculated $^{39}Ar/^{37}Ar$ ratios are over-dispersed with an MSWD of 15, probably an effect of the low signal intensity

and high rise rate; both effects are poorly quantified by the common uncertainty determination from intercept extrapolation. To give a more realistic representation of the uncertainty of the weighted mean of $(^{39}Ar/^{37}Ar)_{Ca}$ we multiplied the sigma uncertainty with the square-root of the MSWD and Student's *t* for *N*-1 degrees of freedom; see Ludwig (2012) for details. Determined ion beam intensities are provided in the Table S1.

The resulting weighted mean values are $(^{36}Ar/^{37}Ar)_{Ca} = (2.649 \pm 0.014) \times 10^{-4}$, $(^{38}Ar/^{37}Ar)_{Ca} = (3.33 \pm 0.12) \times 10^{-5}$ and $(^{39}Ar/^{37}Ar)_{Ca} = (9.1 \pm 0.28) \times 10^{-4}$. These compare with $(^{36}Ar/^{37}Ar)_{Ca} = (2.702 \pm 0.004) \times 10^{-4}$, $(^{38}Ar/^{37}Ar)_{Ca} = (1.96 \pm 0.08) \times 10^{-5}$ and $(^{37}Ar/^{39}Ar)_{Ca} = (7.02 \pm 0.12) \times 10^{-4}$ in CLICIT (Renne *et al.* 2015).

Conclusions

The average neutron flux was about 1.8 times lower in CLOCIT compared with CLICIT. Production rate ratios of Ar isotopes from Ca and K were similar. We found up to three times higher radial fluence gradients and similar axial fluence gradients. Planar fitting of *J*-values on an irradiation disc resulted in residuals on the order of uncertainty in *J*, but systematic deviations could be recognised. At the current state of the technique, the non-planar component of the reactors neutron flux field becomes resolvable and needs to be accounted for to reach even higher precision and aspiring to the 0.1% goal defined by the EARTHTIME community.

Acknowledgements

We thank two anonymous reviewers and Editor Jacinta Enzweiler for handling the manuscript. D.R. was supported by DFG research scholarship RU 2065/1-1. Instrumentation was funded by NSF grants EAR-9005260, 1322017 and SBR-9601592. Facilities support from the Ann and Gordon Getty Foundation is gratefully acknowledged.

References

Grasty R.L. and Mitchell J.G. (1966)
Single sample potassium-argon ages using the omegatron. **Earth and Planetary Science Letters**, **1**, 121–122.

Kuiper K.F., Deino A., Hilgen F.J., Krijgsman W., Renne P.R. and Wijbrans J.R. (2008)
Synchronizing rock clocks of Earth history. **Science**, **320**, 500–504.

Ludwig K.R. (2012)
User's manual for Isoplot 3.75. **Berkeley Geochronology Center Special Publication**, **5.**

Niespolo E.M., Rutte D., Deino A.L. and Renne P.R. (2017)
Intercalibration and age of the Alder Creek sanidine $^{40}Ar/^{39}$ Ar standard. **Quaternary Geochronology**, **39**, 205–213.

Renne P.R., Knight K.B., Nomade S., Leung K.-N. and Lou T.-P. (2005)
Application of deuteron–deuteron (D–D) fusion neutrons to $^{40}Ar/^{39}Ar$ geochronology. **Applied Radiation and Isotopes**, **62**, 25–32.

Renne P.R., Sprain C.J., Richards M.A., Self S., Vanderkluysen L. and Pande K. (2015)
State shift in Deccan volcanism at the Cretaceous-Paleogene boundary, possibly induced by impact. **Science**, **350**, 76–78.

Rutte D., Pfänder J.A., Koleška M., Jonckheere R. and Unterricker S. (2015)
Radial fast-neutron fluence gradients during rotating $^{40}Ar/^{39}Ar$ sample irradiation recorded with metallic fluence monitors and geological age standards. **Geochemistry Geophysics Geosystems**, **16**, 336–345.

Schickler R. and Reese S. (2017)
Installation of a second CLICIT irradiation facility at the Oregon State TRIGA reactor. **International Group on Research Reactors, Conference Proceedings.**

Schickler R.A., Marcum W.R. and Reese S.R. (2013)
Comparison of HEU and LEU neutron spectra in irradiation facilities at the Oregon State TRIGA® reactor. **Nuclear Engineering and Design**, **262**, 340–349.

Supporting information

The following supporting information may be found in the online version of this article:

Table S1. Ar data for fluorite.

Table S2. Ar data for K-rich glass.

This material is available from: http://onlinelibrary.wiley.com/doi/10.1111/ggr.12217/abstract (This link will take you to the article abstract).

